Merging Undergraduate and Graduate Fluid Mechanics through the use of the SIMPLE Method for the Incompressible Navier-Stokes Equations*

CHRISTOPHER DEPCIK and DENNIS ASSANIS
The University of Michigan, 1231 Beal Avenue, 2032 W. E. Lay Automotive Laboratory, Ann Arbor, MI 48109, USA. E-mail: depcikc@umich.edu; assanis@umich.edu

Undergraduate fluid mechanics courses typically deal with the analytical or integral solutions for the governing equations of motion. The shift to graduate fluid mechanics frequently corresponds to the use of the differential equations of motion and their subsequent solution using computational means. Often there is a disconnect in regards to the problems when moving to the higher level courses. The goal of this paper is to provide a connecting thread between the two levels of learning. This is accomplished by comparing one-dimensional (1-D) and two-dimensional (2-D) simulations of the Plane Poiseuille, Plane Couette and Couette-Poiseuille problems against their analytical solutions. For the incompressible Navier-Stokes equations relevant to these problems, the Semi-Implicit Method for Pressure-Linked Equations (SIMPLE) is utilized as the numerical method. The 1-D SIMPLE method helps to illustrate the 2-D solution algorithm and introduce the reader to pressure correction methods. The end result of the paper is a linking of undergraduate and graduate knowledge through the use of the SIMPLE method in increasing order of complexity.

Keywords: computational; fluid mechanics; Navier-Stokes; pressure-correction; analytical; undergraduate; graduate; incompressible.

INTRODUCTION

UNDERGRADUATE FLUID MECHANICS courses typically deal with the analytical or integral solutions for the governing equations of motion. Using these methods helps illustrate to the students the fundamentals of fluid mechanics through problems that can be solved by hand. This also allows for the use of tests to judge the students' knowledge of the subject. The shift to graduate-level computational fluid dynamics (CFD) courses frequently corresponds to the use of the differential equations of motion and their subsequent solution using computational means. Often there is a disconnect in regards to the problems when moving to the higher level courses. This can be exacerbated when the student moves from one university to another as in the first author's case. In addition, different teaching techniques by instructors can add to the confusion as the student does not have a common thread between the two levels of learning. While not all of these issues can be readily alleviated, this paper poses a way to bridge some of the gap between undergraduate and graduate fluid mechanics using simple fundamental problems.

In undergraduate courses, students are first introduced to the concept of internal fluid flow (or pipe flow) through the Plane Poiseuille [1–6], Plane Couette [7–13] and Couette-Poiseuille problems. These problems have one-line analytical answers that help explain to the student the concepts of pressure differences, velocity profiles, shear stresses and laminar flow. At first glance, the use of advanced numerical techniques to solve these problems appears to be an overkill. However, these fundamental problems can provide a common thread between the levels of learning while providing nice and neat solutions to compare and contrast. Verifying numerical methods against known results is a useful way for increasing the level of confidence of a correctly programmed solution. This merging of analytical and numerical problems is not a new concept with Chow's introductory book in CFD a prime example of this technique [14]. This paper builds on that earlier work by including the advanced concepts of pressure-correction, staggered grids along with dimensional reduction and source terms.

In this paper, the differential governing equations of mass and momentum (Navier-Stokes) are first given in compressible two-dimensional (2-D) format. They are then simplified via the incompressible assumption for use with low velocity flows (M < 0.3) and constant density fluids pertinent for the Plane Poiseuille, Plane Couette and Couette-Poiseuille problems. They will then be simplified into one-dimensional (1-D) format including source terms to account for relevant

phenomena. Numerical methods are then illustrated for the 1-D equations as a precursor to a full 2-D solver. Often the 1-D formulation of a numerical method helps to explain the steps needed for the 2-D equations; i.e. most two- and three-dimensional solvers are based off a one-dimensional numerical algorithm [15].

A simple ordinary differential equation solver is first presented for a steady-state solution of the 1-D method to give an introduction into the field of Computational Fluid Dynamics. Then a commonly used pressure correction method, Semi-Implicit Method for Pressure-Linked Equations (SIMPLE) [16–20], is described to solve for the transient version of the 1-D equations. This SIMPLE method is then extended into the second-dimension to provide a full 2-D solver of the incompressible Navier-Stokes equations of mass and momentum. After the description of the methods, simulation of the Plane Poiseuille, Plane Couette and Couette-Poiseuille problems are accomplished using the pertinent 1-D and 2-D numerical algorithms and compared against the analytical solutions. A subsequent problem of Driven Cavity Flow is then modeled as a sample of continuation of concepts in fluid mechanics. In all cases, numerical models, boundary conditions and assumptions are noted for reproduction by the reader.

GOVERNING EQUATIONS

In this section, the two-dimensional (2-D) governing equations of motion (Navier-Stokes) for compressible flow are first simplified via the incompressible assumption for use with low velocity flows (M < 0.3) and constant density fluids. They are then simplified into one-dimensional (1-D) format in order to increase their solution speed and help explain numerical algorithms. Since we will be solving the incompressible version of the Navier-Stokes equations, we will not have to solve the energy equation. This is because it can be solved independently of the mass and momentum equations through a decoupling of the differential equations.

The 2-D compressible Navier-Stokes mass and momentum equations are:

$$\frac{\partial \rho}{\partial t} + \frac{\partial (\rho u)}{\partial x} + \frac{\partial (\rho v)}{\partial y} = 0$$

(2-D comp: mass) (1)

$$\frac{\partial (\rho u)}{\partial t} + \frac{\partial \left(\rho u^2 + p + \tau_{xx}\right)}{\partial x} + \frac{\partial \left(\rho uv + \tau_{xy}\right)}{\partial y} = 0$$

(2-D comp: x-mom) (2)

$$\frac{\partial (\rho v)}{\partial t} + \frac{\partial \left(\rho uv + \tau_{yx}\right)}{\partial x} + \frac{\partial \left(\rho v^2 + p + \tau_{yy}\right)}{\partial y} = 0$$

(2-D comp: y-mom) (3)

Quite often, the assumption of a Newtonian fluid is made where the viscous stresses in the above equations are related to the rates of strain as follows:

$$\tau_{xx} = 2\mu \frac{\partial u}{\partial x} + \lambda \left(\frac{\partial u}{\partial x} + \frac{\partial v}{\partial y}\right),$$

$$\tau_{xy} = \tau_{yx} = \mu \left(\frac{\partial u}{\partial y} + \frac{\partial v}{\partial x}\right),$$

$$\tau_{yy} = 2\mu \frac{\partial v}{\partial y} + \lambda \left(\frac{\partial u}{\partial x} + \frac{\partial v}{\partial y}\right)$$

(4)

where μ is the coefficient of viscosity or dynamic viscosity and λ is defined as the second coefficient of viscosity. The combination of μ and λ in the following form is known as the bulk viscosity, k:

$$k = \lambda + \tfrac{2}{3}\mu$$

(5)

If the bulk viscosity is assumed negligible, via the Stokes hypothesis, we get:

$$\lambda = -\tfrac{2}{3}\mu$$

(6)

Simplifying the governing equations of compressible flow for incompressibility ($\rho = \cancel{c}$) results in the following equations:

$$\frac{\partial u}{\partial x} + \frac{\partial v}{\partial y} = 0$$

(2-D incomp: mass) (7)

$$\frac{\partial u}{\partial t} + \frac{\partial u^2}{\partial x} + \frac{1}{\rho}\frac{\partial p}{\partial x} + \frac{\partial (uv)}{\partial y} = \nu \left(\frac{\partial^2 u}{\partial x^2} + \frac{\partial^2 u}{\partial y^2}\right)$$

(2-D incomp: x-mom) (8)

$$\frac{\partial v}{\partial t} + \frac{\partial (uv)}{\partial x} + \frac{\partial v^2}{\partial y} + \frac{1}{\rho}\frac{\partial p}{\partial y} = \nu \left(\frac{\partial^2 v}{\partial x^2} + \frac{\partial^2 v}{\partial y^2}\right)$$

(2-D incomp: y-mom) (9)

In order to get this form of the incompressible momentum equations, the continuity Equation (7) is substituted within the shear stress terms (4) when converting.

For fast calculation of the 2-D incompressible equations, frequently they are simplified to 1-D. However, in order to capture the correct flow phenomena, source terms need to be added to these equations. The 1-D incompressible equations for mass and momentum including these source terms are:

$$\frac{\partial u}{\partial x} = \frac{S_{mass}}{\rho}$$

(1-D incomp: mass) (10)

$$\frac{\partial u}{\partial t} + \frac{\partial u^2}{\partial x} + \frac{1}{\rho}\frac{\partial p}{\partial x} = \frac{4\nu}{3}\frac{\partial^2 u}{\partial x^2} + \frac{S_{mom}}{\rho}$$

(1-D incomp: x-mom) (11)

where S_{mass} and S_{mom} explain pertinent phenomena in the compressible equations like source/sinks of mass and friction [21, 22]. In order to get to this formulation, the momentum equation does not utilize the continuity Equation (10) in the shear stress terms as before. Instead, the shear stress terms remain as they are written in Equation (4).

As discussed in a previous paper [22], the momentum source term for the 1-D compressible equations accounting for friction (or no slip walls) is equal to:

$$S_{mom} = -\rho \frac{f_F u|u|}{2} \frac{A_s}{V} \qquad (12)$$

For laminar (Re < 2300), fully-developed *pipe* flow, the Darcy friction factor [23] written with Moody subscript [24] is equal to:

$$f_M = \frac{64}{Re} \qquad (13)$$

where:

$$Re = \frac{\rho u d}{\mu} \qquad (14)$$

However, the friction factor used in pipe flow calculations for the momentum source term in Equation (12) is the Fanning friction factor [25]:

$$f_F = \frac{f_M}{4} \qquad (15)$$

Later, in the Examples section, this source term will be adjusted to account for the fact that we will not be modeling pipe flow. This is because we will be assuming that the *z*-direction goes to infinity based on the analytical problems reproduced. Hence, there is no effect on the flow pattern from the wall in this direction. In pipe flow, this is not the case and the origin of the above momentum source term takes this *z*-direction into account through a derivation using cylindrical polar coordinates [26].

Often, the time-scales of velocity are usually small in comparison to the other flow phenomena. As a result, the steady-state formulation of the 1-D incompressible equations can be used:

$$\frac{du}{dx} = \frac{S_{mass}}{\rho}$$

$$(\text{1-D incomp ss: mass}) \qquad (16)$$

$$\frac{dp}{dx} = \frac{4\mu}{3} \frac{d^2u}{dx^2} - 2uS_{mass} + S_{mom}$$

$$(\text{1-D incomp ss: x-mom}) \qquad (17)$$

These equations also provide a simple way of checking the steady-state solution of the transient formulation in Equation (11). In addition, the numerical method described in this paper is for the steady-state solution through continual iteration involving the time-derivative in the x-momentum equation.

NUMERICAL SOLVERS

In the previous section, we simplified the governing equations moving from the highest level of description to the lowest; i.e. 2-D transient to 1-D steady-state. The reason for doing so is to help illustrate the evolution of these simpler formulations. In this section, we document the numerical solvers for incompressible versions of the 1-D and 2-D mass and momentum equations in the reverse order of description, that is, 1-D steady-state to 2-D transient. This is because the numerical algorithms involved often increase in complexity as the level of the equations becomes more complete. In addition, often the 1-D formulation of the numerical method helps to explain the steps needed for the 2-D equations, that is, most two- and three-dimensional solvers are based off a one-dimensional numerical algorithm [15].

One-dimensional steady-state solver

The 1-D steady-state solution of the incompressible mass and momentum equations can be solved in an Euler explicit [27, 28] manner for first-order accuracy in space. Using this method and solving for the velocity and pressure utilizing a backward difference for the differential operators equals:

$$u_i = u_{i-1} + \frac{S_{mass_i}}{\rho}\Delta x \qquad (18)$$

$$p_i = p_{i-1} + S_{prs_i}\Delta x \qquad (19)$$

where:

$$S_{prs_i} = \frac{4\mu}{3}\left(\frac{u_{i+1} - 2u_i + u_{i-1}}{\Delta x^2}\right) - 2u_i S_{mass_i} + S_{mom_i} \qquad (20)$$

utilizes a central-difference operator for the viscous term as described in [29]. This numerical method is acceptable only if the source terms do not become too large and the algorithm becomes unstable. (In order to determine this stability criterion, a von Neumann analysis would need to be completed involving the source terms.) The boundary conditions for this solver are:

$$u|_{i=1} = u_{in} \quad \text{and} \quad p|_{i=1} = p_{in} \qquad (21)$$

As the reader can see, using the Euler explicit method for this set of equations is quite simple to understand and program into a computer. If there are no source terms, the solution is trivial with the velocity and pressure constant across the numerical domain. This method can be used as an introduction into the realm of computational fluid dynamics and is relevant for both undergraduate and graduate courses. It does not require advanced algorithms or complicated grids to compute velocity and pressure profiles.

One-dimensional SIMPLE method

When we look to solve the transient momentum,

Equation (11), we find that we need to incorporate a more complex numerical algorithm. In this paper, we use a pressure-correction technique which utilizes estimates of pressure within the momentum equation in order to solve for the velocity profile [30]. In this method, only the correct pressure distribution will allow the velocity field to satisfy the continuity equation. A commonly used pressure-correction method is the Semi-Implicit Method for Pressure-Linked Equations (SIMPLE) algorithm which has been used since the early 1970s for solution of the 2-D incompressible equations with good accuracy [16–20]. This method uses the time-dependent momentum governing equations to solve for the steady-state solution through continual iteration. We first begin by illustrating this method for the 1-D transient incompressible equations to help describe the method and make it easier for the student to understand.

In the 1-D SIMPLE method, the actual pressure and velocity are replaced with estimated and correction values:

$$p = p^* + p' \quad \text{and} \quad u = u^* + u' \qquad (22)$$

where p^* and u^* are the estimated variables while p' and u' are the correction variables. As a result, the governing equations can be rewritten using these estimated and correction variables:

$$\frac{\partial u^*}{\partial x} + \frac{\partial u'}{\partial x} = S^*_{mass} + S'_{mass} \qquad (23)$$

$$\frac{\partial u^*}{\partial t} + \frac{\partial u'}{\partial t} + \frac{\partial (u^*)^2}{\partial x} + \frac{\partial (u')^2}{\partial x} + \frac{1}{\rho}\left[\frac{\partial p^*}{\partial x} + \frac{\partial p'}{\partial x}\right] =$$

$$\frac{4\nu}{3}\left[\frac{\partial^2 u^*}{\partial x^2} + \frac{\partial^2 u'}{\partial x^2}\right] + \frac{S^*_{mom} + S'_{mom}}{\rho} \qquad (24)$$

It is important to note that the source terms also need to be converted into estimated and correction values because we will solve the estimated and correction equations separately.

The *first* step in the SIMPLE method is to assume a pressure profile p^* within the computational grid. The *second* step is to split the momentum equation into two separate equations (estimated and correction):

$$\frac{\partial u^*}{\partial t} + \frac{\partial (u^*)^2}{\partial x} + \frac{1}{\rho}\left(\frac{\partial p^*}{\partial x}\right) = \frac{4\nu}{3}\left(\frac{\partial^2 u^*}{\partial x^2}\right) + \frac{S^*_{mom}}{\rho}$$

(momentum*) $\qquad (25)$

$$\frac{\partial u'}{\partial t} + \frac{\partial (u')^2}{\partial x} + \frac{1}{\rho}\left(\frac{\partial p'}{\partial x}\right) = \frac{4\nu}{3}\left(\frac{\partial^2 u'}{\partial x^2}\right) + \frac{S'_{mom}}{\rho},$$

(momentum) $\qquad (26)$

and then solve the (momentum*) equation for u^* over the entire domain with the source term a function of u^* and p^*.

The *third* step in the method is to calculate the velocity and pressure correction variables by combining the (momentum') and mass equations into a Poisson equation for pressure. Often in the literature, we find that the velocity correction equation derived from (momentum') equation (26) drops the flux and viscous terms for simplicity:

$$\rho\frac{\partial u'}{\partial t} = -\frac{\partial p'}{\partial x} + S'_{mom} \qquad (27)$$

Since the SIMPLE method uses iterative convergence, neglecting these terms will have no bearing on the final result. It just may take the method somewhat longer to converge because the correction values are not strictly conservative with respect to the governing equations.

Taking a first-order time-derivative of this equation and making the assumption that the velocity correction at the previous time-step is equal to zero because the solution has converged, we get:

$$u' = \frac{\Delta t}{\rho}\left(S'_{mom} - \frac{\partial p'}{\partial x}\right) \qquad (28)$$

Now, taking the derivative of this equation with respect to x we recover:

$$\frac{\partial u'}{\partial x} = \frac{\Delta t}{\rho}\left(\frac{\partial S'_{mom}}{\partial x} - \frac{\partial^2 p'}{\partial x^2}\right) \qquad (29)$$

Substituting the mass conservation equation (23) for the $\partial u'/\partial x$ term in the above equation results in the following Poisson equation for the pressure correction:

$$\frac{\partial^2 p'}{\partial x^2} = \frac{\rho}{\Delta t}\left(\frac{\partial u^*}{\partial x} - S^*_{mass} - S'_{mass}\right) + \frac{\partial S'_{mom}}{\partial x} \quad (30)$$

We now solve for the velocity and pressure correction variables in an iterative manner because the source terms could be a function of u' and p'. If there are no source terms, the pressure correction equation can be solved first and then used within Equation (28) to determine the velocity correction. The *final* step involves updating the variables through equation (22) and iterating until a desired convergence criterion is met.

One-dimensional SIMPLE collocated grid

Ideally, when writing the discretized solution of the SIMPLE algorithm, central difference methods for the flux (convective) terms would be preferred because of their second-order spatial accuracy. However, researchers have found two issues when formulating the method in this manner [29]. The first problem is because of an odd-even decoupling of the equations in which the physical solution is superimposed by oscillatory spurious solutions. This can be solved by adding higher-order artificial dissipation terms to damp the high-frequency errors (see [31]). The second problem is from the elimination of the time derivative of density which causes an additional uncoupling in the centrally discretized equations when applied to

finite volume (difference) meshes. This can result in mass conservation errors and oscillations in the solution. In order to circumvent these issues, this paper describes two solution algorithms for the 1-D case in preparation for the 2-D solution. The first method uses an upwind algorithm on a collocated grid originally determined by Bernard and Thompson [32] whereas the second method uses the more traditional staggered grid method first proposed by Harlow and Welch [33] and often used for the 2-D SIMPLE method. Since the idea of the staggered grid may be new to the reader, the collocated grid method is described first to help with the solution procedure.

Using the collocated grid illustrated in Fig. 1, the second step of the SIMPLE method involves solving for the velocity component u^* after guessing the pressure (p^*) at each grid point:

$$u_i^* = u_i + \Delta t \left[\frac{4\nu}{3} \frac{(u_{i+1} - 2u_i + u_{i-1})}{\Delta x^2} + \frac{S_{mom_i}^*}{\rho} - \frac{(u_{i+1}^2 - u_i^2)}{\Delta x} - \frac{(p_i^* - p_{i-1}^*)}{\rho \Delta x} \right] \quad (31)$$

In this case, the velocity at the previous time-step is equal to the previous guess and the source term is computed implicitly for stability. In the Bernard and Thompson paper, the flux term is not included because they did not include source terms; hence, the velocity is constant in the domain and this term disappears. In this paper, the solution algorithm is written in a general manner to account for any manner of source term and velocity does not need to be constant.

Because of the numerical method, the boundary conditions of this equation involve specifying the exit velocity and not the inlet velocity from the upwind differenced flux term. This is because the flux term is the important finite-difference that propagates the flow whereas the viscous term involves only a secondary damping effect. In addition, since the viscous term is central-differenced, we will need to include a boundary condition for the inlet, that is, the solution of this equation is over the domain $i = 2$ to $N_x - 1$. As a result, the boundary conditions for this equation equal:

$$\left. \frac{du^*}{dx} \right|_{i=1} = S_{mass}^* \big|_{i=1} \quad \text{and} \quad u_{N_x}^* = u_{outlet} \quad (32)$$

In this case, we utilize a steady-state equation for the boundary conditions in order to eliminate the need for a time-dependent algorithm. It is important to mention that the boundary conditions for the estimated pressure follow in a similar manner to the estimated velocity but the inlet pressure can be specified because of the difference direction:

$$p_1^* = p_{inlet} \quad \text{and} \quad \left. \frac{dp^*}{dx} \right|_{i=N_x} = S_{prs}^* \big|_{i=N_x} \quad (33)$$

Continuing the finite difference in the above manner, we find that the Poisson equation for the pressure correction is equal to:

$$p_i' = \frac{p_{i+1}' + p_{i-1}'}{2} - \frac{\Delta x}{2}$$

$$\left\{ \frac{\rho}{\Delta t} \left[(u_{i+1}^* - u_i^*) - S_{mass_i}^* - S_{mass_i}' \right] + \frac{S_{mom_{i+1}}' - S_{mom_{i-1}}'}{2} \right\} \quad (34)$$

Since a central difference is utilized for the pressure correction, boundary conditions have to be determined for $i = 1$ and N_x. These are similar to the boundary conditions for the estimated pressure, Equation (33), but specification of the inlet pressure at this boundary requires the pressure correction to be equal to zero:

$$p_1' = 0 \quad \text{and} \quad \left. \frac{dp'}{dx} \right|_{i=N_x} = S_{prs}' \big|_{i=N_x} \quad (35)$$

After calculating the pressure correction over the entire domain, the velocity correction can be computed as:

$$u_i' = \frac{\Delta t}{\rho} \left[S_{mom_i}' - \frac{(p_i' - p_{i-1}')}{\Delta x} \right] \quad (36)$$

with the boundary conditions computed similarly to the estimated velocity and the pressure correction:

$$\left. \frac{du'}{dx} \right|_{i=1} = S_{mass}' \big|_{i=1} \quad \text{and} \quad u_{N_x}' = 0 \quad (37)$$

New values for the pressure and velocity are then computed from the estimated and correction values with an under-relaxation constant included in the pressure solution:

$$p = p^* + \alpha p' \quad \text{and} \quad u = u^* + u' \quad (38)$$

This under-relaxation constant $(0 < \alpha \leq 1)$ is needed because it has been found that the pressure correction equation tends to overestimate its value whereas the velocity correction values are reasonable [29]. To complete the solution procedure, p and u are set equal to p^* and u^* and iteration is repeated until convergence is found at each time-step.

One-dimensional SIMPLE staggered grid

Since the flux term in the estimated velocity equation for the collocated grid method does not take into account the entrance velocity from the upwind differencing, this numerical discretization is not the preferred solution procedure. Instead, researchers tend to use a staggered grid, illustrated in Fig. 2, where the velocity is defined on the ½ grid (empty circles) and p is defined on the i grid (filled circles). Staggered grids allow for a better coupling of the variables and also improve the
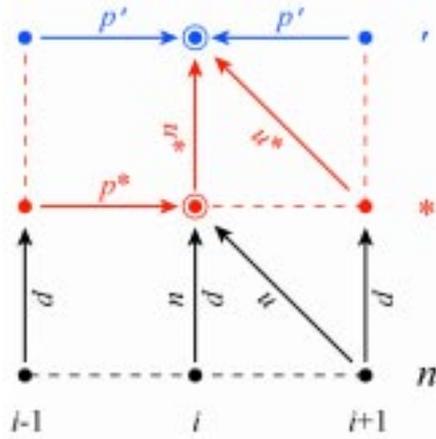
Fig. 1. SIMPLE 1-D collocated grid illustrating the variable solution paths taken.

stability of the system of equations. In addition, they permit the programmer use of central difference schemes in order to increase accuracy to second-order and, in our case, specification of an inlet velocity.

For the 1-D staggered grid example that follows, we discretize the equations with the pressure on the grid and the velocity on the ½ grid. Therefore, in order to compute the value for the velocity on the pressure grid, an average quantity is used:

$$u_i = \frac{1}{2}\left(u_{i-\frac{1}{2}} + u_{i+\frac{1}{2}}\right) \qquad (39)$$

The staggered grid is utilized when solving for the estimated velocity because the ½ grid values of velocity must be taken into account:

$$u^*_{i+\frac{1}{2}} = u_{i+\frac{1}{2}} + \Delta t \left[\frac{4\nu}{3}\frac{\left(u_{i+\frac{3}{2}} - 2u_{i+\frac{1}{2}} + u_{i-\frac{1}{2}}\right)}{\Delta x^2}\right.$$

$$\left. + \frac{S^*_{mom_{i+\frac{1}{2}}}}{\rho} - \frac{\left(u^2_{i+\frac{3}{2}} - u^2_{i-\frac{1}{2}}\right)}{2\Delta x} - \frac{\left(p^*_{i+1} - p^*_i\right)}{\rho\Delta x}\right] \qquad (40)$$

In this case, a second-order central derivative is used for the flux term in comparison to the first-order upwind derivative in Equation (31). Since the grid is defined for pressure, ghost cells for velocity are needed in order to complete the solution domain. The inlet velocity is defined as the entrance ghost cell, whereas the steady-state equation for the velocity is utilized at the exit. Because the exit ghost cell occurs after the computational domain, the source term is no longer valid there and is therefore calculated at the last point in the domain:

$$u^*_{\frac{1}{2}} = u_{inlet} \quad \text{and} \quad \left.\frac{du^*}{dx}\right|_{i=N_x+\frac{1}{2}} = S^*_{mass}\big|_{i=N_x} \qquad (41)$$

The boundary conditions for the pressure are computed as before in Equation (33) because of the pressure grid. The finite difference format of the Poisson equation for the pressure correction now includes the ½ grid velocity and source term variables due to the staggered mesh.

$$p'_i = \frac{p'_{i+1} + p'_{i-1}}{2} - \frac{\Delta x}{2}\left\{\frac{\rho}{\Delta t}\left[\left(u^*_{i+\frac{1}{2}} - u^*_{i-\frac{1}{2}}\right) - \right.\right.$$

$$\left.\left. S^*_{mass_{i+\frac{1}{2}}} - S'_{mass_{i+\frac{1}{2}}}\right] + \left(S'_{mom_{i+\frac{1}{2}}} - S'_{mom_{i-\frac{1}{2}}}\right)\right\} \qquad (42)$$

with the boundary conditions the same as Equation (35). The velocity correction also reflects the staggered grid:

$$u'_{i+\frac{1}{2}} = \frac{\Delta t}{\rho}\left[S'_{mom_{i+\frac{1}{2}}} - \frac{\left(p'_{i+1} - p'_i\right)}{\Delta x}\right] \qquad (43)$$

with the following ghost cells computed similar to the estimated velocity ghost cells:

$$u'_{\frac{1}{2}} = 0 \quad \text{and} \quad \left.\frac{du'}{dx}\right|_{i=N_x+\frac{1}{2}} = S'_{mass}\big|_{i=N_x} \qquad (44)$$

Fig. 2. SIMPLE 1-D staggered grid illustrating the variable solution paths taken for (a) velocity and (b) pressure.
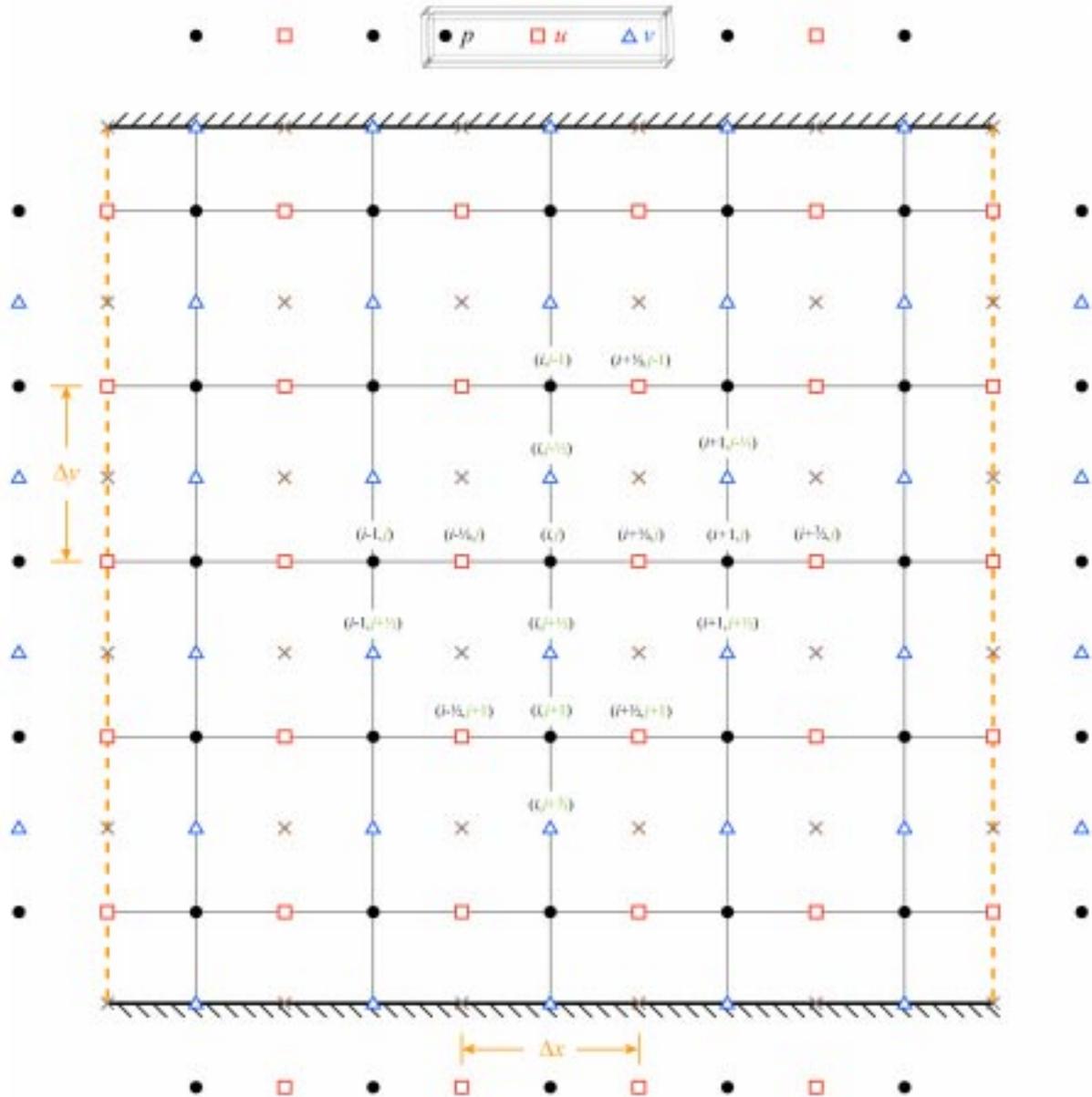
Fig. 3. Staggered grid schematic for 2-D flow.

Equation (38) completes the solution algorithm and an iterative procedure can be used until convergence of the pressure and velocity domain.

When calculating the time-step to use within the algorithm, the Courant and diffusive stability conditions are combined:

$$\Delta t \leq \min\left(\frac{\Delta x}{|u_{\max}|}, \frac{\Delta x^2}{4\nu}\right) \qquad (45)$$

This value is just a guideline as the source term can affect the stability of the system. Reduction in the time-step and/or under-relaxation constant can be done if the solution is unable to converge.

The uses of source terms within the 1-D SIMPLE solvers are needed to account for phenomena such as wall friction. These components can add to the confusion of the numerical method and may be omitted when first discussing pressure-correction techniques in a classroom setting. They can be included after the initial discussion of the method to illustrate to the students why source terms are important and how they can be incorporated within the solver. The use of estimated and correction values of the source terms is also important when the situation arises where they are needed in the two-dimensional method presented in the next section. The 1-D methods presented can then be referenced to illustrate how they can be incorporated correctly within this pressure-correction technique.

Two-dimensional SIMPLE solver

As mentioned in the Introduction, we often find that 2-D numerical methods are formulated the same as their 1-D counterparts. In the following

paragraphs, the 2-D SIMPLE method is shown to follow the exact same algorithm as the 1-D SIMPLE method. In the 2-D case, the pressure and *x*-velocity terms are again split according to Equation (22) with the *y*-velocity split similarly:

$$v = v^* + v' \qquad (46)$$

The governing equations reflect this incorporation as illustrated here by the mass equation (now ignoring source terms):

$$\frac{\partial u^*}{\partial x} + \frac{\partial u'}{\partial x} + \frac{\partial v^*}{\partial y} + \frac{\partial v'}{\partial y} = 0 \qquad (47)$$

We now have two *x*-momentum and *y*-momentum equations each, divided into estimated and correction variables. The correction variable formulation of the momentum equations is used to calculate the *u* and *v* velocity correction equations like the 1-D method; see equation (27):

$$\rho\frac{\partial u'}{\partial t} = -\frac{\partial p'}{\partial x} \quad \text{and} \quad \rho\frac{\partial v'}{\partial t} = -\frac{\partial p'}{\partial y} \qquad (48)$$

Again, the flux terms are omitted in order to simplify the method. Now, taking a first-order time derivative and making a similar assumption to the 1-D case with respect to the previous time-step, we get the equations for the velocity corrections; see equation (28):

$$u' = -\frac{\Delta t}{\rho}\frac{\partial p'}{\partial x} \quad \text{and} \quad v' = -\frac{\Delta t}{\rho}\frac{\partial p'}{\partial y} \qquad (49)$$

Similar to the 1-D method, taking derivatives of the above equations with respect to *x* and *y*, adding the results and substituting the equation for mass (47), we recover the Poisson equation for pressure correction:

$$\frac{\partial^2 p'}{\partial x^2} + \frac{\partial^2 p'}{\partial y^2} = \frac{\rho}{\Delta t}\left(\frac{\partial u^*}{\partial x} + \frac{\partial v^*}{\partial y}\right) \qquad (50)$$

The 2-D solution procedure follows the 1-D case by first assuming a pressure profile, p^*, across the numerical domain. In the second step, the *x*- and *y*-momentum* equations are solved for u^* and v^*:

$$\frac{\partial u^*}{\partial t} + \frac{\partial (u^*)^2}{\partial x} + \frac{1}{\rho}\frac{\partial p^*}{\partial x} + \frac{\partial (u^*v^*)}{\partial y} = \nu\left(\frac{\partial^2 u^*}{\partial x^2} + \frac{\partial^2 u^*}{\partial y^2}\right)$$

$$(\text{*x*-momentum*}) \qquad (51)$$

$$\frac{\partial v^*}{\partial t} + \frac{\partial (u^*v^*)}{\partial x} + \frac{\partial (v^*)^2}{\partial y} + \frac{1}{\rho}\frac{\partial p^*}{\partial y} = \nu\left(\frac{\partial^2 v^*}{\partial x^2} + \frac{\partial^2 v^*}{\partial y^2}\right)$$

$$(\text{*y*-momentum*}) \qquad (52)$$

In the staggered grid arrangement, the time-deri-

vatives in the above equations are written in a first-order manner:

$$\frac{\partial u}{\partial t} = \frac{u^*_{i+\frac{1}{2},j} - u_{i+\frac{1}{2},j}}{\Delta t}$$

and

$$\frac{\partial v}{\partial t} = \frac{v^*_{i,j+\frac{1}{2}} - v_{i,j+\frac{1}{2}}}{\Delta t} \qquad (53)$$

whereas, the flux terms are written as second-order central difference operators:

$$\frac{\partial (u^*)^2}{\partial x} = \frac{u^2_{i+\frac{3}{2},j} - u^2_{i-\frac{1}{2},j}}{2\Delta x}$$

and

$$\frac{\partial (u^*v^*)}{\partial y} = \frac{(uv)_{i+\frac{1}{2},j+1} - (uv)_{i+\frac{1}{2},j-1}}{2\Delta y} \qquad (54)$$

$$\frac{\partial (v^*)^2}{\partial y} = \frac{v^2_{i,j+\frac{3}{2}} - v^2_{i,j-\frac{1}{2}}}{2\Delta y}$$

and

$$\frac{\partial (u^*v^*)}{\partial x} = \frac{(uv)_{i+1,j+\frac{1}{2}} - (uv)_{i-1,j+\frac{1}{2}}}{2\Delta x} \qquad (55)$$

The viscous derivatives are also written using a second-order central difference methodology:

$$\frac{\partial^2 u^*}{\partial x^2} = \frac{u_{i+\frac{3}{2},j} - 2u_{i+\frac{1}{2},j} + u_{i-\frac{1}{2},j}}{\Delta x^2}$$

and

$$\frac{\partial^2 u^*}{\partial y^2} = \frac{u_{i+\frac{1}{2},j+1} - 2u_{i+\frac{1}{2},j} + u_{i+\frac{1}{2},j-1}}{\Delta y^2} \qquad (56)$$

$$\frac{\partial^2 v^*}{\partial x^2} = \frac{v_{i+1,j+\frac{1}{2}} - 2v_{i,j+\frac{1}{2}} + v_{i-1,j+\frac{1}{2}}}{\Delta x^2}$$

and

$$\frac{\partial^2 v^*}{\partial y^2} = \frac{v_{i,j+\frac{3}{2}} - 2v_{i,j+\frac{1}{2}} + v_{i,j-\frac{1}{2}}}{\Delta y^2} \qquad (57)$$

The pressure derivatives are written in a first-order difference manner as traditionally found in the literature (a second-order central difference formulation will also work):

$$\frac{\partial p^*}{\partial x} = \frac{p^*_{i+1,j} - p^*_{i,j}}{\Delta x} \quad \text{and} \quad \frac{\partial p^*}{\partial y} = \frac{p^*_{i,j+1} - p^*_{i,j}}{\Delta y} \qquad (58)$$

In the third step, the Poisson equation for pressure (50) is solved for the correction pressure according to the following pressure and velocity derivatives:

$$\frac{\partial^2 p'}{\partial x^2} = \frac{p'_{i+1,j} - 2p'_{i,j} + p'_{i-1,j}}{\Delta x^2}$$

and

$$\frac{\partial^2 p'}{\partial y^2} = \frac{p'_{i,j+1} - 2p'_{i,j} + p'_{i,j-1}}{\Delta y^2} \quad (59)$$

$$\frac{\partial u^*}{\partial x} = \frac{u^*_{i+\frac{1}{2},j} - u^*_{i-\frac{1}{2},j}}{\Delta x}$$

and

$$\frac{\partial v^*}{\partial y} = \frac{v^*_{i,j+\frac{1}{2}} - v^*_{i,j-\frac{1}{2}}}{\Delta y} \quad (60)$$

The velocity correction variables, u' and v', are then solved according to Equation (49) with the following first-order derivatives:

$$\frac{\partial p'}{\partial x} = \frac{p'_{i+1,j} - p'_{i,j}}{\Delta x}$$

and

$$\frac{\partial p'}{\partial y} = \frac{p'_{i,j+1} - p'_{i,j}}{\Delta y} \quad (61)$$

Finally, the variables are updated according to Equation (38) and a similar expression for the y-velocity:

$$v = v^* + v' \quad (62)$$

and the iterative procedure is repeated until a desired convergence is met. The time-step criterion now includes the second dimension:

$$\Delta t \leq \min\left(\frac{\Delta x}{|u_{\max}|}, \frac{\Delta y}{|v_{\max}|}, \frac{\Delta x^2}{4\nu}, \frac{\Delta y^2}{4\nu}\right) \quad (63)$$

In the 2-D case, the staggered grid can be interpreted in a number of ways according to what variables the user wishes to define at the boundaries. In Fig. 3, a staggered grid is illustrated for a problem of flow between two parallel plates; the crosses in the figure show a collocated grid configuration. In this figure, the x-velocity grid points are set at the inflow and outflow boundaries and the y-velocity grid points are set at the upper and lower plates. In the following sections, the boundary conditions are illustrated in the figures of the different problems to document what was used by the authors.

In this section, we documented the numerical algorithms that are used within this paper. The goal was to illustrate how the complexity of the methods multiplies as the level of description increases. In the following sections, simple problems of fluid flow are solved according to the computational methods described. These solutions are compared to the analytical solutions found in undergraduate fluid dynamics textbooks. The idea is to demonstrate to the reader how the level of information in undergraduate and graduate courses can be merged to continue the advance-

ment of the student while remaining consistent with their previous experience. In addition, these historical problems provide a good methodology for proving that the numerical methods have been programmed correctly.

PLANE POISEUILLE FLOW

In fluid dynamics courses, it is common to discuss problems involving fluid flow within pipes as illustrated in Fig. 4. In these examples, concepts such as laminar and turbulent flow can be discussed along with other phenomena such as shear stress, head loss and velocity profiles. One of the first examples given to undergraduate students when trying to explain internal flow is fully-developed laminar flow between infinite parallel plates often referred to as the Plane Poiseuille or Hagen-Poiseuille problem.

The origination of this problem stems from Dr. Jean Leonard Marie Poiseuille's contribution to laminar flow phenomena in 1846 [6] with preliminary reports found earlier in the literature [2-5]. In a translated version of the work [34], the editor mentions that this paper was the first important contribution in the field in regards to the knowledge of viscous flow and the data captured from the setup in Fig. 5 is among the best available for determining the viscosity of water. Dr. Poiseuille was primarily concerned about studying the flow of blood within the arteries, veins and capillaries for medical reasons. His work ended up becoming one of the pioneering efforts in the area of hydraulic flow. It was later suggested by Wolfgang Ostwald [35, 36] that this problem should be renamed the Hagen-Poiseuille problem because earlier in 1839 Gotthilf Hagen had come to the same conclusions as Poiseuille using the setup in Fig. 6 [1]. However, it was mentioned by the editor of [34] that his conclusions were less convincing than what Poiseuille found.

In the Poiseuille and Hagen setups, pressure directs the flow through a small gap which can then be modeled as flow between infinite plates as illustrated in Fig. 7. The plates are considered infinite in the z-direction with no variation of any fluid property in this direction. The flow is assumed to be steady and incompressible and according to the problem description, the pressure gradient in the x-direction must be finite to balance the shear forces. However, both walls will affect the y-direction gradient to the same degree, so dp/dy can be considered to be zero. The velocity distribution in the liquid between the plates is parabolic at infinite time and found analytically to be equal to [26]:

$$u = \frac{d^2}{2\mu}\left(\frac{\partial p}{\partial x}\right)\left[\left(\frac{y}{d}\right)^2 - \left(\frac{y}{d}\right)\right] \quad (64)$$

At the point of maximum velocity, the x-velocity
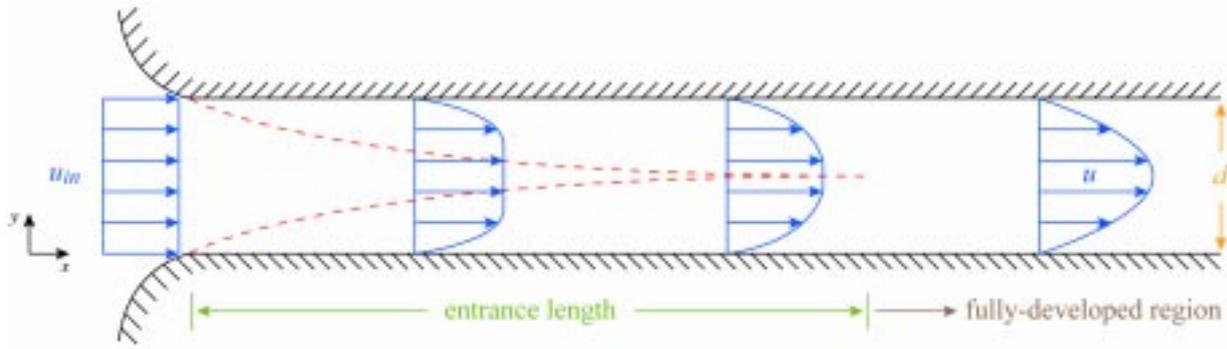
Fig. 4. Developing flow in a pipe.
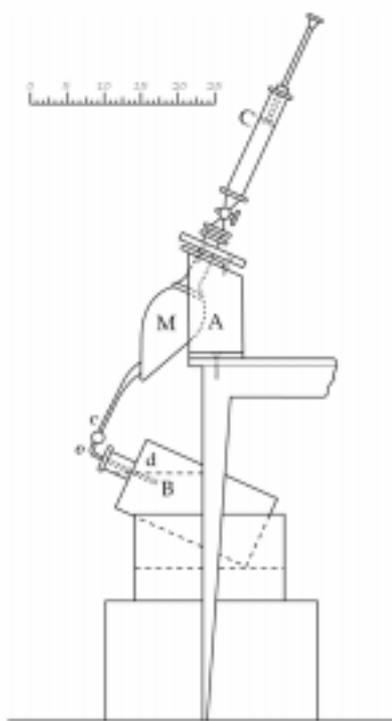
Fig. 5. Reproduced diagram of Poiseuille's experimental setup [34].
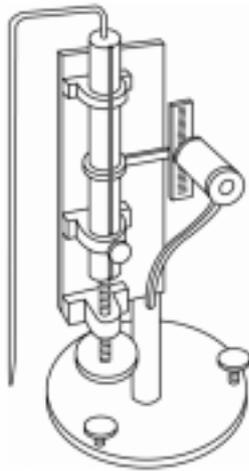
Fig. 6. Reproduced diagram of Hagen's experimental setup [1].

derivative in the *y*-direction is equal to zero (du/dy) and the above relationship becomes:

$$u_{\max} = -\frac{1}{8\mu}\left(\frac{\partial p}{\partial x}\right)d^2 = \frac{3}{2}u_{in} \qquad (65)$$

Utilizing these two equations, the normalized velocity profile is written as:

$$\frac{u}{u_{\max}} = -4\left[\left(\frac{y}{d}\right)^2 - \left(\frac{y}{d}\right)\right] \qquad (66)$$

The distance downstream from the entrance where the flow can be considered to be fully-developed is referred to as the *entrance length* and is approximately equal to:

$$\frac{L_{ent}}{d} \approx 0.06\frac{\rho u_{in}d}{\mu} \qquad (67)$$

The analytical solutions of the problem illustrate that there is a pressure profile in the *x*-direction and a velocity profile in the *y*-direction. In a 1-D simulation, the velocity profile cannot be determined because we assume that the cross-sectional velocity is constant. However, source terms can be used to calculate the pressure drop as a function of distance. In accordance with our earlier description of the frictional source term in the momentum equation, see Equation (12), we were able to determine a source term from the analytical analysis that is relevant for fully-developed laminar flow between parallel plates:

$$S_{mom} = -12\mu\frac{|u|}{d^2} \qquad (68)$$

It is important to note that in many simulations, the pressure drop is the more important characteristic to determine because of energy constraints; i.e. backpressures in the exhaust of internal combustion engine.

In the 2-D case, the velocity and pressure profiles can be computed and compared directly with the analytical solutions. The boundary conditions for the flow profile illustrated in Fig. 7 are straightforward with regards to the inlet and plates. In specific, we are assuming that the inlet
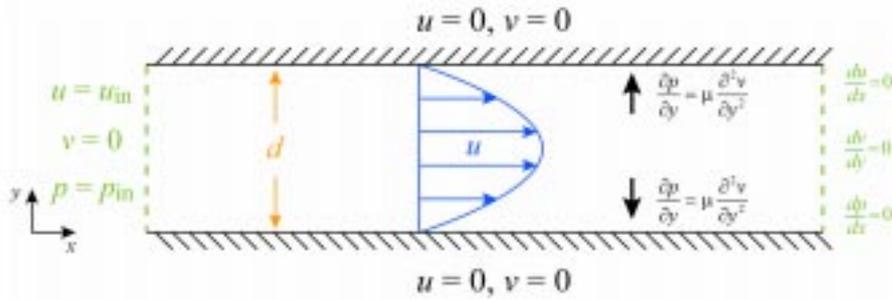
Fig. 7. Schematic of flow and pertinent boundary conditions for Plane Poiseuille or Hagen-Poiseuille flow.

velocity and pressure are known and the velocity is normal to the inlet face. The no slip velocity condition is employed at the upper and lower plates with both velocity values equal to zero. The pressure condition at the plates is found by analyzing the y-momentum Equation (9) and utilizing the no slip condition; i.e. all terms drop out except for the pressure derivative and the viscous component in the y-direction. This is because $du/dx = 0$ from the no slip condition

and $dv/dy = 0$ from the mass equation. However, $\partial^2 v/\partial y^2$ does not necessarily have to be equal to zero.

For the outflow conditions, we assume that du/dx is equal to zero which then requires dv/dy being equal to zero from the continuity equation. For the pressure, we assume that dp/dx is equal to zero [37] but this is not completely correct. According to Harlow and Welch [33], the pressure boundary condition at the free surface should be derived
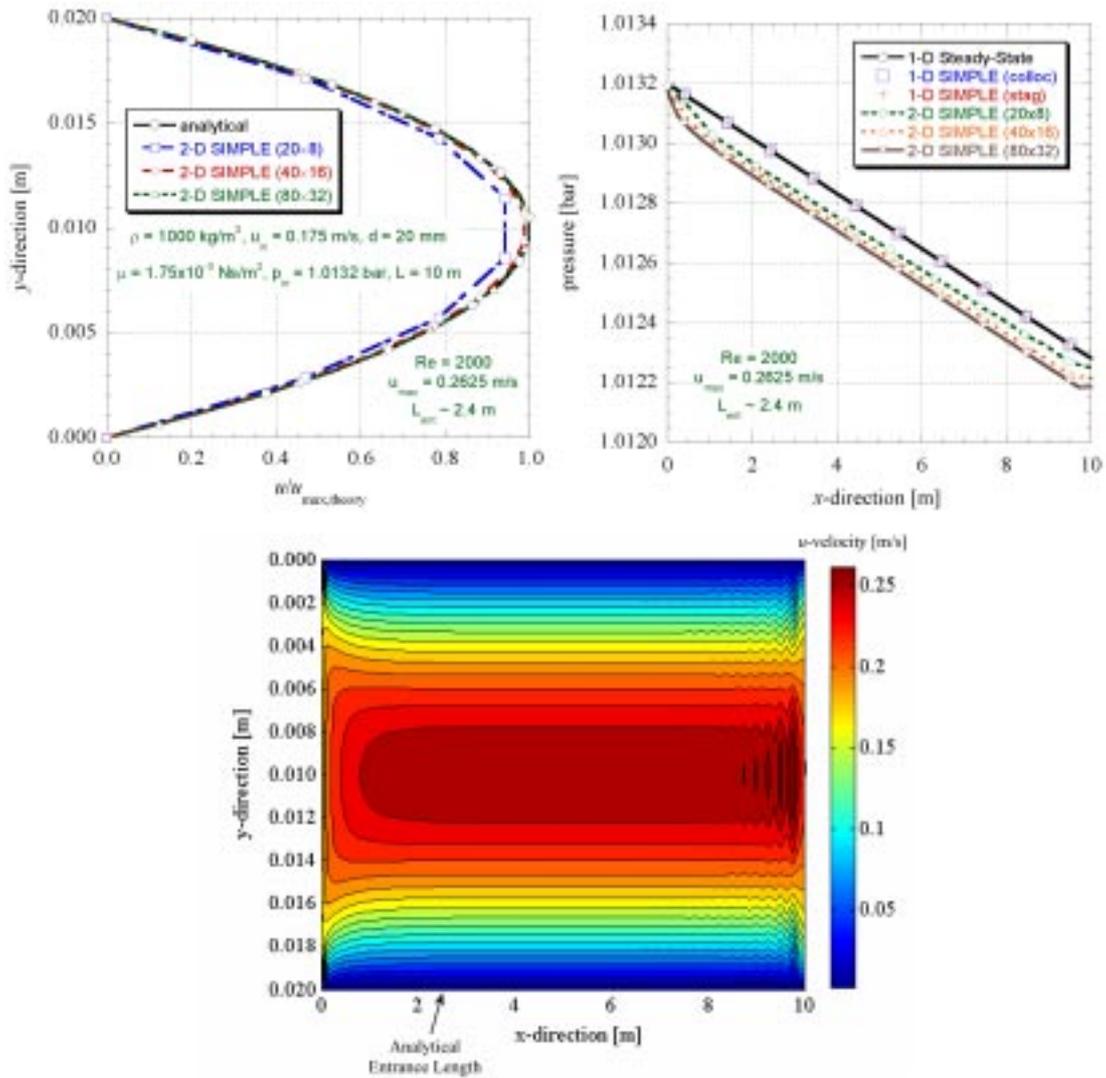
Fig. 8. Analytical, 1-D and 2-D solutions of the Plane Poiseuille velocity and pressure profiles.

from the requirement of vanishing normal stress component. They mention that there are two reasons why this condition is difficult to apply accurately. For the first reason, the normal stress components can be calculated only if surface orientation is known which may be hard to do using a finite difference representation. This is not the case for our grid as we have a simple rectangular grid where the outlet orientation is well defined. The second reason has to do with our assumptions for velocity that hold consistent to the equation of mass. They state these velocity derivatives give fairly accurate results, however they do not necessarily give the proper viscous stress at the exit.

In Fig. 8, the analytical, 1-D collocated and staggered and 2-D results are given for an example calculation with a Reynolds number equal to 2000. For the 1-D solution, both collocated and staggered grids give the same pressure drop as the analytical solution. In the 2-D solution, the simulation predicts the same velocity profile as the analytical case with increasing accuracy based on larger grid sizes. The pressure drop in the 2-D case deviates slightly as the contour plot of the 80×32

grid illustrates that there is a slight oscillation at the exit. This has to do with our assumptions for the boundary conditions at the exit as explained in the previous paragraph. The contour plot also illustrates that the predicted entrance length of the simulation is close to what is estimated analytically. This is shown by the velocity holding constant after about 2.5 m until the exit boundary conditions affect the flow. Overall, 1-D and 2-D simulations can model this simple flow pattern based on the level of description that is needed.

PLANE COUETTE FLOW

In this section, another commonly used problem in undergraduate fluid mechanics courses is solved using the 2-D SIMPLE method. In this problem, fully-developed laminar flow is encountered when a liquid is sheared between two coaxial cylinders. This was originally found by Maurice Marie Alfred Couette [38] using the setup of Fig. 9 and explained in a number of papers [7–9, 12, 13] and a condensed version [10] of his doctoral thesis [11]. Because the clearance gap is small and symmetric,
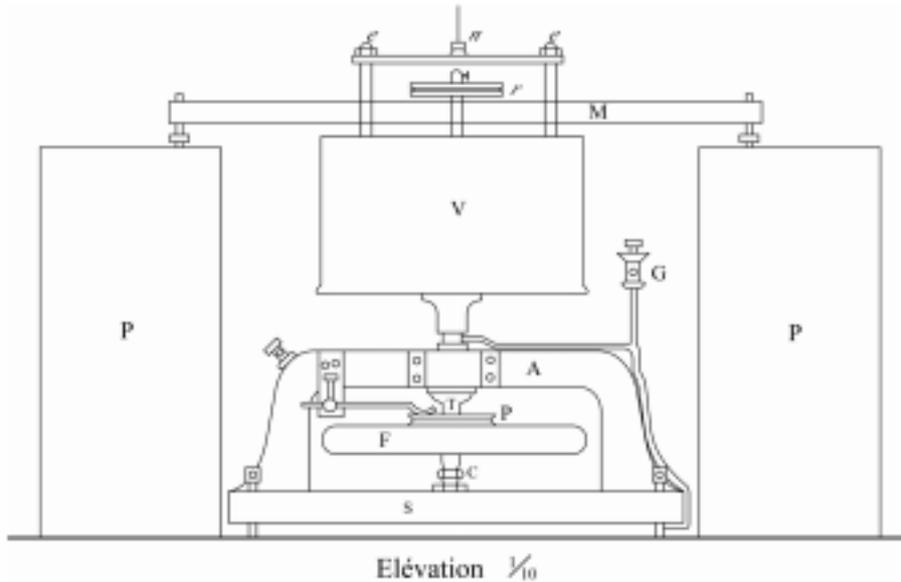
Fig. 9. Reproduced diagram of Couette viscometer [10].
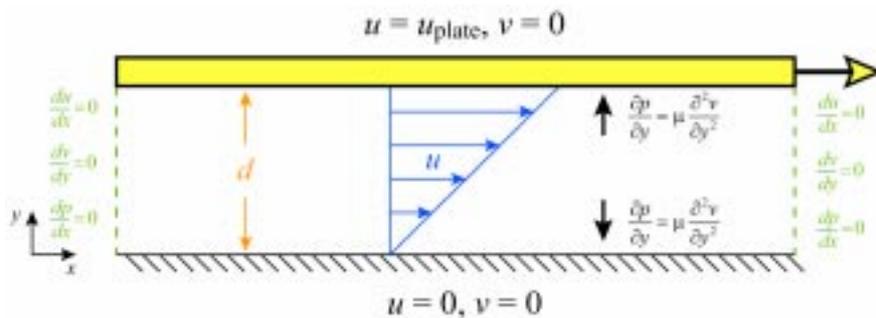
Fig. 10. Schematic of flow and pertinent boundary conditions for the Plane Couette problem.
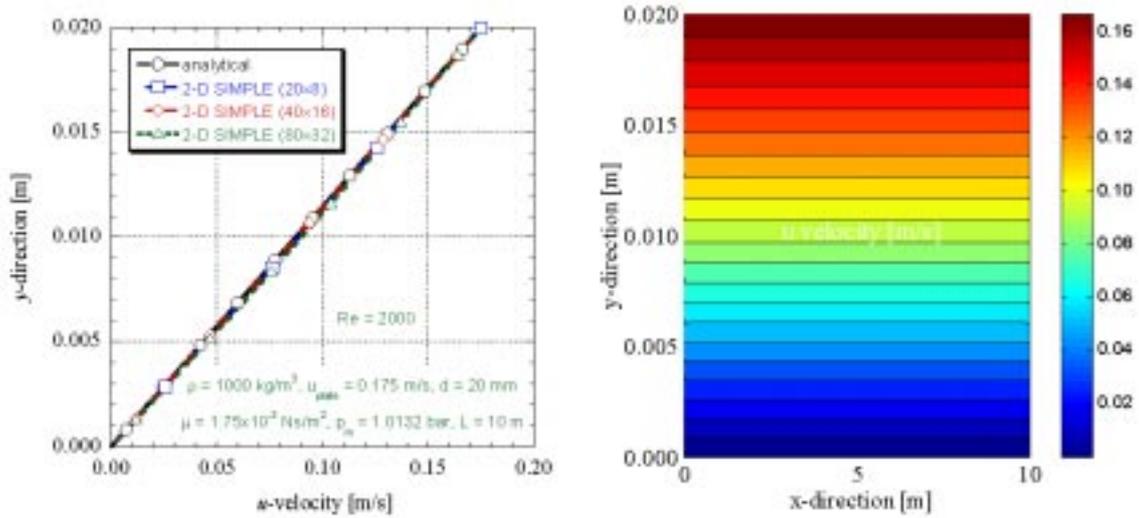
Fig. 11. Analytical and 2-D SIMPLE solutions of the Plane Couette flow problem.
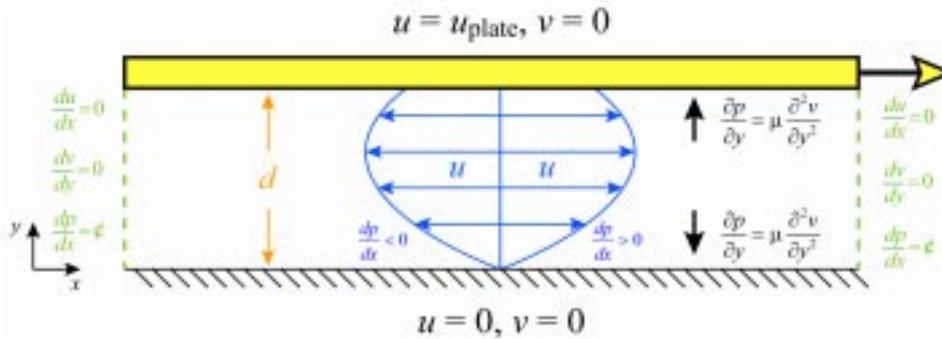
Fig. 12. Schematic of flow and pertinent boundary conditions for the Couette-Poiseuille problem.

this problem can be converted into one involving flow between infinite parallel plates where the upper plate is moving with constant speed [26].

In the previous example, the flow of the fluid in the pipe caused a velocity and pressure profile to be evident. However, in this case the fluid motion is caused by the movement of the upper plate as illustrated in Fig. 10. Because of this, there is not any externally imposed pressure gradient $(dp/dx = 0)$ and we do not need to worry about solving for the pressure. A simple analytical analysis can again be used to calculate a velocity distribution of the following linear profile [26]:

$$u = \frac{u_{\text{plate}}}{d} y \qquad (69)$$

In many ways the solution of this problem is trivial, as shown in Fig. 11, and using a 2-D algorithm to reproduce it could be considered overkill. However, if the reader is having issues programming the staggered grid and/or the solutions do not appear to be correct, they can use this problem to eliminate the pressure dependence from the algorithm (no need to solve the Poisson equation) and make sure that the velocity equations are programmed correctly. In addition, it also helps reinforce previous lessons learned in

undergraduate education with a graduate level analysis. Note that the 1-D governing equations can only be used to simulate the pressure gradient, so this problem cannot be simulated using 1-D numerical algorithms.

COUETTE-POISEUILLE FLOW

Often the lessons in undergraduate courses continue through a combination of the Plane Couette and Plane Poiseuille problems. In this case, the upper plate is moving with flow occurring between the plates as illustrated in Fig. 12. The analytical velocity distribution for this Couette-Poiseuille problem ends up being a summary of the previous results of Equations (64) and (69) [26]:

$$u = \frac{d^2}{2\mu} \left(\frac{\partial p}{\partial x} \right) \left[\left(\frac{y}{d} \right)^2 - \left(\frac{y}{d} \right) \right] + u_{plate} \left(\frac{y}{d} \right) \qquad (70)$$

Again, the solution is trivial as seen in Fig. 13, and the need to simulate it using a complicated 2-D numerical method may be unnecessary. However, because this problem incorporates a pressure profile which can be specified by the user (in our
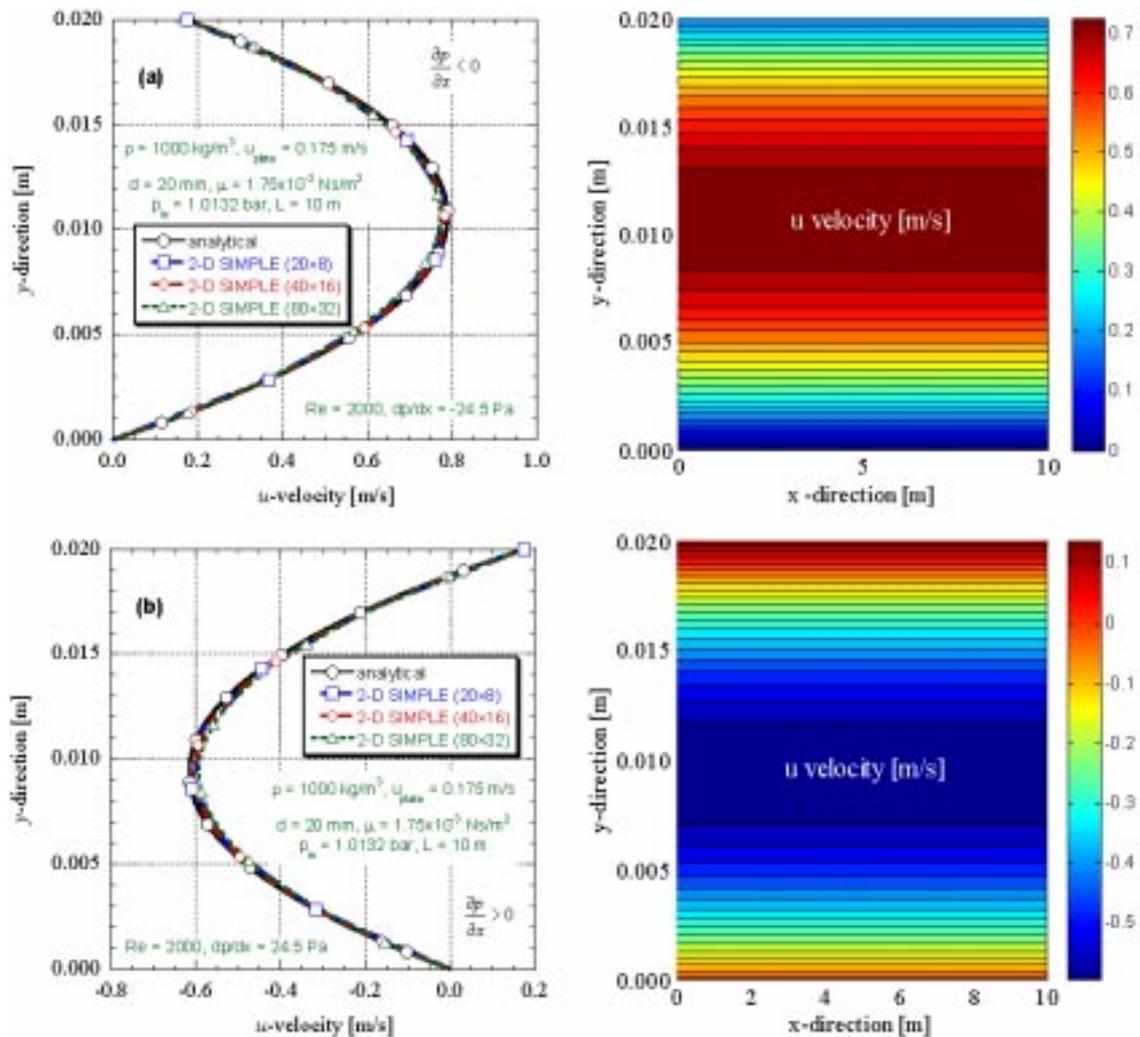
Fig. 13. Analytical and 2-D SIMPLE solutions of the combined Couette-Poiseuille problem for (a) dp/dx = –24.5 Pa and (b) dp/dx = 24.5 Pa.

case ±24.5 Pa), it allows for the programmer to determine whether or not the pressure terms in the momentum equations have been incorporated correctly. Utilizing this problem along with the Plane Couette problem allows for complete verification of the velocity fields without having to incorporate the Poisson equation for pressure. This also has the benefit of increasing the run time of the simulation and decreasing the complexity of the solver.

DRIVEN CAVITY FLOW

At this point, if the reader is able to reproduce all of the previous example problems they should be confident that they have programmed the numerical codes correctly. They can then move onto other problems of fluid mechanics to help illustrate other pertinent fluid fundamentals. In this section, the primitive variable formulation of the 2-D governing equations is compared to the streamfunction-vorticity formulation. The stream-

function (ψ) and vorticity (ω) version of the incompressible Navier-Stokes equations has the main benefit of reducing the number of governing equations by one. In addition, the basic numerical algorithm is easier to understand and the solution results better illustrate flow phenomena like the streamlines across an airplane wing. The main problem with this method is the incorporation of the boundary conditions which can be confusing. However, comparing and contrasting the primitive formulation with the $\psi - \omega$ equations can help enlighten the student as how to comprehend these boundary conditions.

One problem that is often reproduced using the $\psi - \omega$ formulation is the driven cavity flow problem illustrated in Fig. 14. This is possibly the simplest example that can be reproduced because it does not contain inflow or outflow sections. In this problem, flow inside the box is driven by a plate moving at a constant velocity. The boundary conditions are easy to understand with all velocities equal to zero at the boundaries except for the u velocity of the moving plate. In an educational
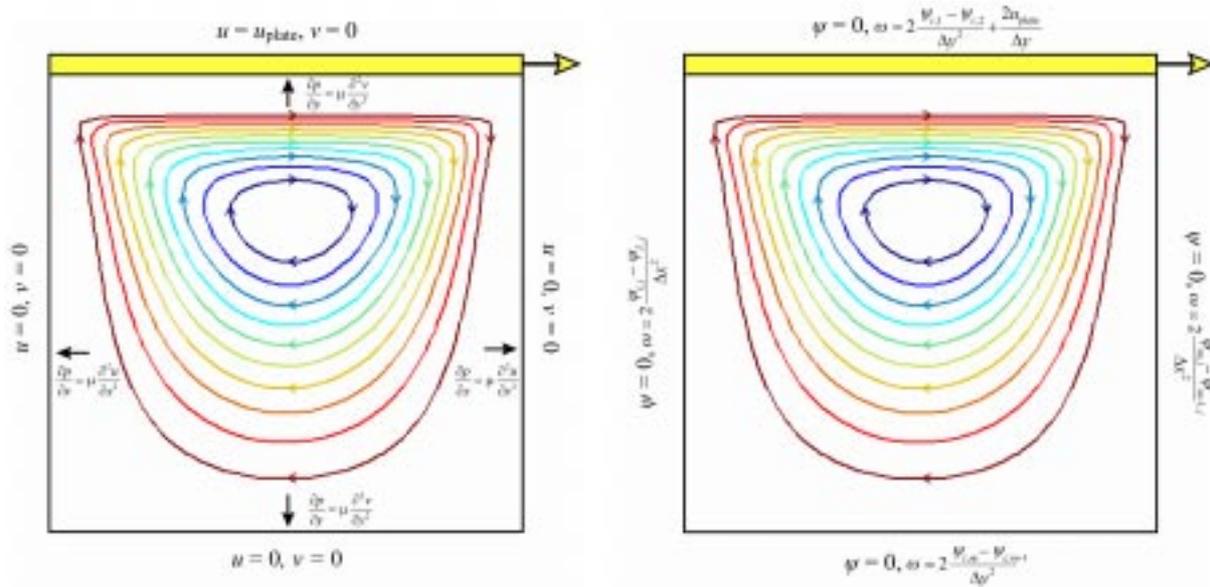
Fig. 14. Driven cavity flow problem illustrating boundary conditions for primitive and streamfunction-vorticity variables.
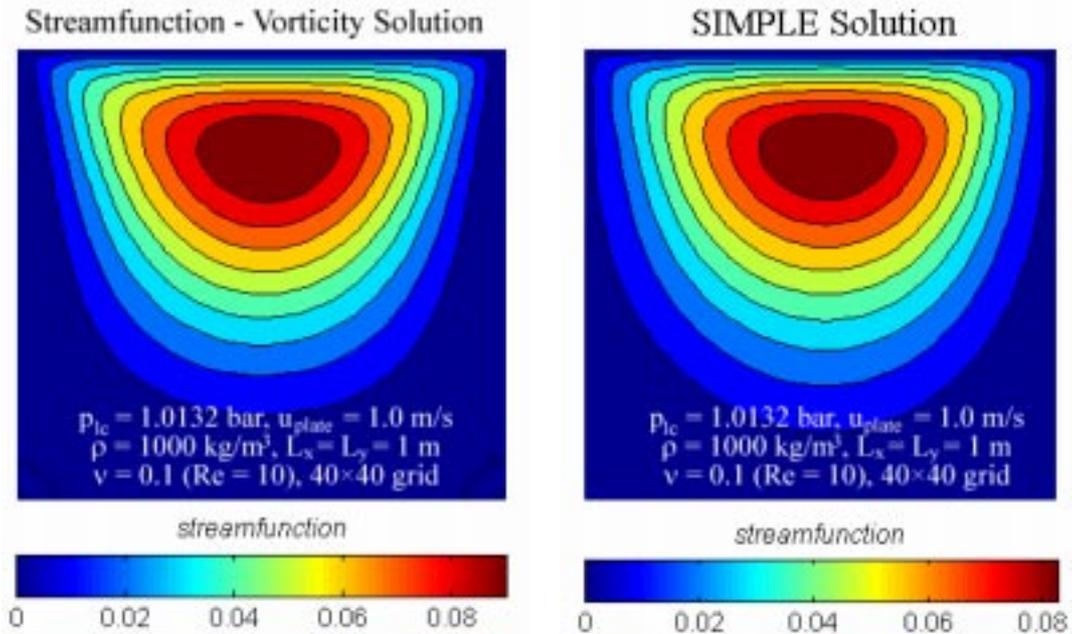
Fig. 15. Comparison of streamfunction plots for the streamfunction-vorticity and SIMPLE solvers.

setting, utilizing this problem helps the student learn about changing the system of variables and different solution techniques. It builds on the previously utilized knowledge in this paper without confronting the student with a blank slate.

The vorticity and streamfunction variables are defined as:

$$\omega = \frac{\partial v}{\partial x} - \frac{\partial u}{\partial y} \qquad (71)$$

$$u = \frac{\partial \psi}{\partial y} \quad \text{and} \quad v = -\frac{\partial \psi}{\partial x} \qquad (72)$$

Using these definitions can simplify the incompressible mass and momentum equations of motion to be equal to:

$$\frac{\partial^2 \psi}{\partial x^2} + \frac{\partial^2 \psi}{\partial y^2} = -\omega \qquad (73)$$

$$\frac{\partial \omega}{\partial t} + u\frac{\partial \omega}{\partial x} + v\frac{\partial \omega}{\partial y} = \nu\left(\frac{\partial^2 \omega}{\partial x^2} + \frac{\partial^2 \omega}{\partial y^2}\right) \qquad (74)$$

The solution of these equations was previously published in a paper illustrating the use of Graphical User Interfaces (GUIs) in an educational setting [39]. In Fig. 15, the streamfunction solu-

tions are given for both the ψ-ω and primitive version of the equations. For the primitive version, the streamfunction was computed using equation (72) in an upwind manner to compare directly with the ψ-ω solution. The results show a good agreement between the two methods with some slight differences because of the variables involved. It is often useful for the instructor to demonstrate a couple different ways of solving the same equations because certain problems may benefit by using another technique.

CONCLUSIONS

The difference between undergraduate and graduate fluid mechanics often comes from the shift from analytical to computational solutions. In order to help ease this transition, this paper illustrates a methodology for building on the fundamentals of undergraduate education in a graduate setting. In specific, the elementary problems of Plane Poiseuille, Plane Couette and Couette-Poiseuille flow were solved using both analytical and computational methods. The numerical methods utilized began with 1-D ordinary differential equations and moved in increasing complexity until the solution of 2-D partial differential equations. Finally, the problem of driven cavity flow was solved to illustrate a way to build on the knowledge presented to further a student's education of computational methods.

Utilizing the numerical methods presented in this paper, instructors will be able to demonstrate the following concepts to students:

- grid independence and numerical convergence;
- pressure-correction techniques and the effect of their corresponding parameters (α);
- 1-D and 2-D numerical methods and their problem relevance;
- boundary conditions, ghost cells and their effect on the solution;
- ordinary and partial differential equations;
- primitive variable and streamfunction-vorticity Navier-Stokes incompressible equations.

One main benefit of this paper is the use of the 1-D equations of motion to demonstrate how to solve a pressure-correction algorithm. In specific, the use of a reduced degree of freedom method helps to deconstruct the basic steps needed for multi-dimensional flow. This can be used to help the student better understand the method without unnecessarily confusing the situation.

It can be said that the problems modeled in this paper are trivial in nature and advanced numerical techniques are not needed for their solution. While this may be so, these simple problems help bridge the gap between undergraduate and graduate education. They provide one-line solutions to prove the correct implementation of the numerical methods. They also inform the student of the history of hydraulics and where the early advances were made.

REFERENCES

1. G. Hagen, Ueber die Bewegung des Wassers in engen cylindrischen Röhren, *Poggendorff's Annalen der Physik und Chemie*, **46**, 1839, pp. 423–442.
2. J. L. M. Poiseuille, Recherches expérimentelles sur le mouvement des liquides dans les tubes de très petits diamètres, *Comptes Rendus Hebdomadaires des Séances de L'Académie des Sciences*, **11**, 1840, pp. 961–967.
3. J. L. M. Poiseuille, Recherches expérimentelles sur le mouvement des liquides dans les tubes de très petits diamètres, *Comptes Rendus Hebdomadaires des Séances de L'Académie des Sciences*, **11**, 1840, pp. 1041–1048.
4. J. L. M. Poiseuille, Recherches expérimentales sur le mouvement des liquides dans les tubes de très petits diamètres, *Comptes Rendus Hebdomadaires des Séances de L'Académie des Sciences*, **12**, 1841, pp. 112–115.
5. J. L. M. Poiseuille, Experimentelle Untersuchungen über die Bewegung der Flüussigkeiten in Röhren von sehr kleinen Durchmesser, *Poggendorff's Annalen der Physik und Chemie*, **58**, 1843, pp. 424–448.
6. J. L. M. Poiseuille, Recherches expérimentales sur le mouvement des liquides dans les tubes de très petits diamètres, *Mémoires présentés par divers savans à l'Académie royale des sciences de l'Institut de France: Sciences mathématiques et physiques*, **9**, 1846, pp. 433–545.
7. M. M. A. Couette, Oscillations tournantes d'un solide de révolution en contact avec un fluide visqueux, *Comptes Rendus des Séances de l'Académie des Sciences*, **105**, 1887, pp. 1064–1067.
8. M. M. A. Couette, Sur un nouvel appareil pour l'étude du frottement des fluids, *Comptes Rendus des Séances de l'Académie des Sciences*, **107**, 1888, pp. 388–390.
9. M. M. A. Couette, La viscosité des liquides, *Bulletin des Sciences Physiques de la Faculté des Sciences de Paris*, **4**, 1888, pp. 40–62, 123–133, 262–278.
10. M. M. A. Couette, Études sur le frottement des liquides, *Annales de Chimie et de Physique*, serie VI, **21**, 1890, pp. 433–510.
11. M. M. A. Couette, Études sur le Frottement des Liquides, *Doctorat ès-sciences Physiques Faculté des Sciences de Paris*, **119**, 1890.
12. M. M. A. Couette, Distinction de deux régimes dans le mouvement des fluides, *J. Physique*, série 2, **IX**, September 1890, pp. 414–424.
13. M. M. A. Couette, Corrections relatives aux extrémités des tubes dans la méthode de Poiseuille, *J. Physique*, série 2, IX, December 1890, pp. 560–562.

14. C.-Y. Chow, *An Introduction to Computational Fluid Mechanics,* Seminole Publishing Company, Boulder, Colorado (1983).
15. B. van Leer, Upwind-difference methods for aerodynamic problems governed by the euler equations: large-scale computations in fluid mechanics, *Lectures in Applied Mathematics.* **22**(2), 1985, pp. 327–336.
16. L. S. Caretto, et al., Two calculation procedures for steady, three-dimensional flows with recirculation, *Lecture Notes in Physics* (1972) pp. 60–68.
17. S. V. Patankar, Numerical prediction of three-dimensional flows, *Studies in Convection: Theory, Measurement and Applications,* Academic, New York (1975) pp. 1–78.
18. S. V. Patankar, A calculation procedure for two-dimensional elliptic situations, *Numerical Heat Transfer,* **4**, 1981, pp. 409–425.
19. S. V. Patankar and D. B. Spalding, A calculation procedure for heat, mass and momentum transfer in three-dimensional parabolic flows, *Int. J. Heat and Mass Transfer,* **15**, 1972, pp. 1787–1806.
20. G. D. Raithby and G. E. Schneider, Numerical solution of problems in incompressible fluid flow: treatment of the velocity-pressure coupling, *Numerical Heat Transfer,* **2**, 1979, pp. 417–440.
21. C. Depcik and D. Assanis, One-dimensional automotive catalyst modeling, *Progress in Energy and Combustion Science,* **31**(4), 2005, pp. 308–369.
22. C. Depcik, B. van Leer and D. Assanis, The numerical simulation of variable-property reacting-gas dynamics: new insights and validation, *Numerical Heat Transfer,* Part A, **47**, 200, pp. 27–56.
23. H. Darcy, *Recherches Expérimentales Relatives au Mouvement de L'Eau dans les Tuyaux,* Mallet-Bachelier, Paris (1857).
24. L. F. Moody, Friction factors for pipe flow, *Trans. American Society of Mechanical Engineering,* **66**, 1944, pp. 671–684.
25. J. T. Fanning, *A Practical Treatise on Water-Supply Engineering,* D. Van Nostrand, New York (1877).
26. R. W. Fox and A. T. McDonald, *Introduction to Fluid Mechanics,* John Wiley & Sons, Inc., New York (1992).
27. A. L. Cauchy, *Leçons sur les Applications du Calcul Infinitésimal à la Géométrie, par M. Imprimerie Royale,* Paris (1826–28).
28. L. Euler, *Institutionum Calculi Integralis,* St. Petersburg (1768).
29. C. Hirsch, *Numerical Computation of Internal and External Flows*, John Wiley & Sons Ltd., New York (1990).
30. J. C. Tannehill, D. A. Anderson and R. H. Pletcher, *Computational Fluid Mechanics and Heat Transfer,* Taylor & Francis, Washington (1997).
31. C. M. Rhie and W. L. Chow, Numerical study of the turbulent flow past an airfoil with trailing edge separation, *AIAA Journal,* **21**, 1983, pp. 1525–1532.
32. R. S. Bernard and J. F. Thompson, Mass conservation on regular grids for incompressible flow, *AIAA Paper 84–166* (1984).
33. F. H. Harlow and J. E. Welch, Numerical calculation of time-dependent viscous incompressible flow of fluid with free surface, *The Physics of Fluids,* **8**(12), 1965, pp. 2182–2189 .
34. J. L. M. Poiseuille, *Experimental Investigations Upon the Flow of Liquids in Tubes of Very Small Diameter,* Lancaster Press, Inc., Easton, Pa. (1940).
35. W. Ostwald, Über die geschwindigkeitsfunktion der viskosität disperser system I, *Kolloid-Zeitschrift,* **36**(2), 1925, pp. 99–117.
36. L. Schiller, *Drei klassiker der strömungslehre: Hagen, Poiseuille, Hagenbach,* Herausgegeben von Professor Dr. L. Schiller, Akademische Verlagsgesellschaft M.B.H., Leipzig (1933).
37. K. A. Hoffmann and S. T. Chiang, *Computational Fluid Dynamics: Volume I, Engineering Education System,* Wichita, Kansas (2000).
38. J. M. Piau, et al., Maurice Couette, one of the founders of rheology, *Rheologica Acta,* **33**, 1994, pp. 357–368.
39. C. Depcik and D. Assanis, Graphical user interfaces in an engineering educational environment, *Computer Applications in Engineering Education,* **13**(1), 2005, pp. 48–59.

Christopher Depcik received his BS degree in mechanical engineering from the University of Florida in 1997. He obtained his first MS degree in mechanical engineering in 1999 and his second MS degree in aerospace engineering in 2002 from the University of Michigan. In 2003, he obtained his Ph.D. degree in mechanical engineering from the same university under the supervision of Prof. Dennis Assanis. He is currently a research fellow in the Department of Mechanical Engineering at the University of Michigan. His areas of research involve variable-property reacting-gas dynamics and their application to the exhaust of internal combustion engines including aftertreatment devices. He is also working in the area of fuel reforming and fuel cell simulation. In addition, he is actively involved in developing educational software for engineering courses.

Dennis Assanis is a professor and chair of mechanical engineering and the Jon R. and Beverly S. Holt Professor of Engineering at the University of Michigan, where he is also the director of the Automotive Research Center. He received his B.Sc. degree in marine engineering from the University of Newcastle-upon-Tyne, UK, in 1980. He has received four graduate degrees from the Massachusetts Institute of Technology: SM in naval architecture and marine engineering (1982), SM in mechanical engineering (1982), Ph.D. in power and propulsion (1985), and SM in management (1986). Prior to joining the

University of Michigan in 1994, he was an assistant professor (1985–1990) and an associate professor (1990–1994) in the Department of Mechanical Engineering at the University of Illinois Urbana-Champaign. His research interests include modeling and computer simulation of internal combustion engine processes and systems; experimental studies of engine heat transfer, combustion, and emissions; and automotive systems design optimization. He has published over 150 articles in journals and refereed conference proceedings, and he is a fellow of the Society of Automotive Engineers.